CHEMICAL ENGINEERING TRANSACTIONS
VOL. 69, 2018
A publication of AIDIC
The Italian Association of Chemical Engineering
Online at www.aidic.it/cet
Guest Editors: Elisabetta Brunazzi, Eva Sorensen
Copyright © 2018, AIDIC Servizi S.r.l.
ISBN 978-88-95608-66-2; **ISSN** 2283-9216
DOI: 10.3303/CET1869025

Pilot Tests and Rate-Based Modelling of CO_2 Capture in Cement Plants Using an Aqueous Ammonia Solution

José-Francisco Pérez-Calvo[a], Daniel Sutter[a], Matteo Gazzani[b], Marco Mazzotti[a,*]

[a]Institute of Process Engineering, ETH Zurich (Switzerland)
[b]Copernicus Institute of Sustainable Development, University of Utrecht (The Netherlands)
marco.mazzotti@ipe.mavt.ethz.ch

A rate-based model for the absorption of CO_2 with aqueous ammonia solutions has been developed on the grounds of new CO_2 absorption experiments performed at pilot plant scale. Tests have been performed with synthetic flue gases reproducing cement plant conditions. A thorough design of experiments has been carried out with the aim of studying the influence of several variables on the CO_2 capture performance and obtaining a reliable model in a broad experimental space. The newly developed rate-based model makes use of a thermodynamic framework that predicts reliably the formation of solids in the CO_2-NH_3-H_2O system in order to avoid operating conditions that lead to clogging of the absorber.

1. Introduction

The Chilled Ammonia Process (CAP) is among the most mature technologies for post-combustion CO_2 capture. The detailed design of the process requires the use of rate-based process simulations. Concerning the absorber, such a model should include both the mass and the heat transfer between the vapor and the liquid, and the reaction kinetics of CO_2 in the liquid phase. While the application of the CAP to natural gas and coal-fired power plants has been validated and demonstrated in various facilities of different scale with CO_2 concentration in the flue gas ranging from 3 to 16 %vol (Baburao et al., 2015), the application of the CAP to cement plants, where the CO_2 concentration can be as high as 35 %vol, has not been investigated yet: The higher partial pressure of CO_2 in the inlet stream will considerably affect the CO_2 absorption unit, leading to different temperature and concentration profiles along the column (Pérez-Calvo et al., 2017) that might be outside the validity range of the available models. Indeed, rate-based models presented in the literature for the CO_2-NH_3-H_2O system have been validated with pilot plant CO_2 absorption tests performed with flue gases containing only up to 12 %vol CO_2 (Qi et al., 2013). Furthermore, most of these models make use of the eNRTL-based thermodynamics available in Aspen Plus (hereinafter referred to as “Chen model”) for the computation of activities (Que and Chen, 2011). Although 4 different solid intermediate compounds may form in the system (Jänecke, 1929), the Chen model only considers ammonium bicarbonate. In this regard, the extended UNIQUAC thermodynamic framework by Darde et al. (2010) (hereinafter referred to as “Thomsen model”) has been proven to describe accurately the experimental evidence regarding solid formation. This makes the Thomsen model better suited to predict criticalities within the CAP so as to find the limits of the operating conditions that avoid solid formation within the process (Sutter et al., 2015). On the other hand, while a generalized correlation to compute the CO_2 mass transfer from the vapor to the liquid phase has been obtained for different type of packings in their application to CO_2 capture using aqueous solutions (Wang et al., 2016), substantial disparities have been found experimentally when measuring the apparent kinetic constant of the reaction of CO_2 with NH_3 in the liquid phase (Yu et al., 2016).

In this work, we show the development of a new rate-based model for the absorption of CO_2 with aqueous NH_3 solutions based upon typical flue gas compositions from cement plants. Consequently, new CO_2 absorption experiments have been performed at pilot plant scale with synthetic flue gases to reproduce the conditions found in cement plants. The new rate-based model uses: (i) the Thomsen model as thermodynamic framework, (ii) a generalized correlation from the literature to compute the CO_2 mass transfer coefficients in the vapor and the liquid phase, as well as the interfacial area (Wang et al., 2016), and (iii) a simplified kinetic

Please cite this article as: Perez-Calvo J.F., Sutter D., Gazzani M., Mazzotti M., 2018, Pilot tests and rate-based modeling of co2 capture in cement plants using an aqueous ammonia solution, Chemical Engineering Transactions, 69, 145-150 DOI: 10.3303/CET1869025

model for the reaction of CO_2 with NH_3 in the liquid phase. The reaction rate parameters of the kinetic model have been regressed using the value of the apparent kinetic constant obtained experimentally in this work. In order to obtain a reliable model, pilot plant tests have been carried out varying several parameters, i.e. the inlet gas CO_2 concentration, the inlet liquid temperature, the liquid-to-gas flowrate ratio, the CO_2 loading and the NH_3 concentration in the inlet liquid stream, as well as the gas velocity in the column.

2. Experimental framework

2.1 Pilot plant

The CO_2 absorption tests have been performed in a pilot plant in order to test the system and fine-tune the model before scaling up. A schematic of the test rig used during the experimental campaigns is shown in Figure 1. The packing of the absorption column is 3 m high, with a diameter of 450 mm. The packing used was Koch Glitsch Flexipac M 350X. Online measurements of the CO_2 and NH_3 concentration in the liquid streams were performed using Fourier Transform Near-Infrared spectroscopy (FT-NIR), while OPSIS gas analyzers were used in the gas streams. A mass-balance tool was used to predict the necessary additions (lean solution, rich solution, ammonia solution, water and drain) to keep the concentration in the tank – and consequently in the liquid at the top of the absorber – invariant over time. Sampling of the absorber inlet and outlet liquid streams was carried out for offline liquid composition determination by titration. For each experiment, average values of the measured variables were computed while the system was at steady state.

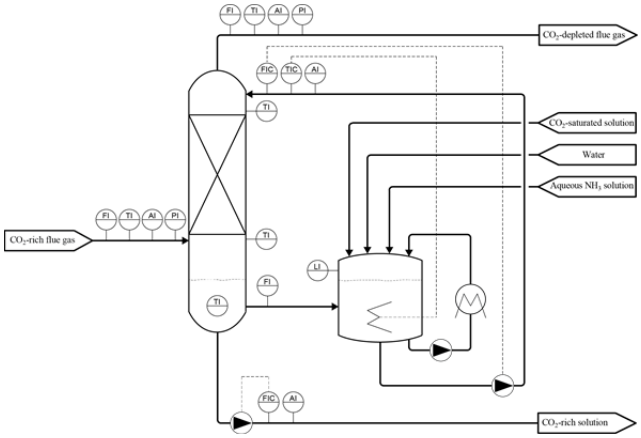

Figure 1: Schematic of the pilot plant used during the CO_2 absorption tests.

2.2 Experimental conditions

Table 1 shows the boundary conditions of the operating variables selected for the tests. Experiments were divided into 3 different types of tests representing the different sections of a real column (Sutter et al., 2015) assuming 90% of CO_2 capture efficiency: (i) tests simulating the bottom part of the industrial absorber where the CO_2 concentration is at its maximum (up to 35 %vol in the case of flue gases from cement plants) and the aqueous ammonia solution has been enriched in CO_2 (Campaign 1); (ii) tests mimicking the middle section of the industrial absorber, right below the feed position of the CO_2-lean stream, where the flue gas has already been partially depleted in CO_2 (Campaign 2); and (iii) experiments reproducing the conditions found at the top of the industrial absorber, where a split stream of the CO_2-rich liquid stream is cooled down and sent to the top of the absorber (often referred to as “pumparound”) to limit the NH_3 slip in the CO_2-depleted flue gas leaving the column (Campaign 3). In comparison with the pilot plant experiments available in the literature (Yu et al., 2011), not only the CO_2 concentration in the inlet flue gas has been increased up to 35 %vol in order to simulate cement plant-like flue gas conditions, but also the experimental range of the liquid NH_3 concentration has been increased from 0-4 to 4-10 molNH_3/kg_{water} in order to test typical operating conditions of the absorber (Sutter et al., 2015). Avoidance of solid formation for all tests was preliminary checked making use of the Thomsen model and confirmed experimentally afterwards. The design of experiments can be seen in Figure 2, where each colored sphere corresponds to one single experiment performed at certain combination of CO_2 partial pressure in the inlet gas stream, and CO_2 loading, NH_3 concentration and temperature in the inlet liquid stream. The experimental space studied for those tests belonging to Campaigns 1 and 2 is shown in Figure 2A), while the tests performed during Campaign 3 are shown in Figure 2B). In addition, repeatability experiments have been carried out.

Table 1: Summary of experimental conditions

Stream	Variable			Campaign 1	Campaign 2	Campaign 3
Inlet liquid	NH_3 concentration	$C_{NH_3}^{in}$	mol_{NH3}/kg_{water}	3.9 – 10.2	4.1 – 10.2	4.1 – 9.6
	CO_2 loading	$l_{CO_2}^{in}$	mol_{CO2}/mol_{NH3}	0.43 – 0.70	0.24 – 0.52	0.46 – 0.61
	Temperature	T_L^{in}	°C	5 – 45	5 – 25	0 - 25
Inlet gas	CO_2 partial pressure	$p_{CO_2,G}^{in}$	kPa	20 – 35	8 – 20	2 – 7
	NH_3 partial pressure	$p_{NH_3,G}^{in}$	kPa	0 – 3	0 – 8	4 – 7
	Superficial velocity	$v_{S,G}^{in}$	m/s	0.7 – 0.9	0.7 – 1.1	0.8 – 0.9
	Temperature	T_G^{in}	°C	10 – 15	10 – 15	10 – 15
Inlet liquid and gas	Liquid-to-gas flowrate ratio	L^{in}/G^{in}	kg/kg	7.5 – 12.0	7.5 – 12.5	2.0 – 3.0

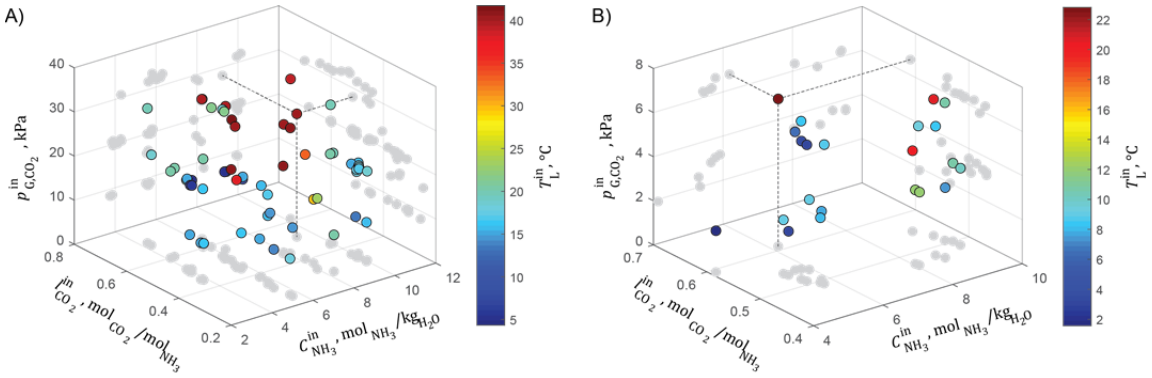

Figure 2: Experimental space studied during the pilot plant tests of the CO_2 absorber: A) Tests of Campaigns 1 and 2; and B) Tests of Campaign 3. The projections of each sphere (experimental point) upon each plane are shown in grey.

3. Model framework

3.1 Thermodynamics

The model takes into account solid-liquid equilibria (SLE) for five different solid phases. The extended UNIQUAC model is used for the computation of the activity coefficients of the species in the liquid phase, while the Soave-Redlich-Kwong equation of state is used to calculate the fugacities in the vapor. The phase diagram for the CO_2-NH_3-H_2O system predicted by the Thomsen model is shown in Figure 3 for typical operating conditions in the absorber.

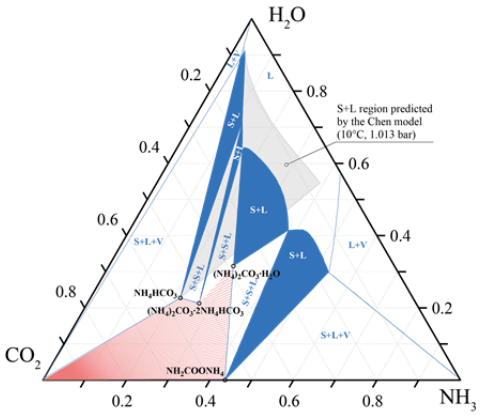

Figure 3: Phase diagram predicted by the Thomsen model (10 °C, 1.013 bar). Compositions are given in weight fractions. S, L and V refer to solid, liquid and vapor phases, respectively. The pure solid compositions are represented by black dots. Additional phase diagrams for the CO_2-NH_3-H_2O system predicted by the Thomsen model at typical operating conditions of the CAP can be found elsewhere (Sutter et al., 2015).

3.2 Reaction kinetics in the liquid phase

The chemical reactions taking place in the aqueous phase are:

$$H_2O \leftrightarrow OH^- + H^+ \quad (1)$$

$$NH_3 + H^+ \leftrightarrow NH_4^+ \quad (2)$$

$$HCO_3^- \leftrightarrow CO_3^{2-} + H^+ \quad (3)$$

$$CO_2 + OH^- \leftrightarrow HCO_3^- \quad (4)$$

$$CO_2 + 2NH_3 \leftrightarrow NH_2COO^- + NH_4^+ \quad (5)$$

Reactions involving the transfer of a proton are considered to reach equilibrium instantaneously. On the contrary, the bicarbonate and carbamate ion formation reactions, i.e. Reaction (4) and Reaction (5), respectively, are kinetically controlled, although Reaction (5) has a predominant impact on the CO_2 absorption rate at typical operating conditions. Nevertheless, different studies have reported substantial disparities in the apparent kinetic constant, and have proposed different reaction mechanisms (Yu et al., 2016). In the case of dilute aqueous ammonia solutions, the reaction rate of Reaction (5) can be simplified to the expression given by Eq(6), an empirical correlation that, although not representing the reaction mechanism, can be used for engineering purposes in equipment design and process optimization.

$$r_{\mathrm{cm}} = k_{\mathrm{cm}} C_{\mathrm{NH_3}}^{n} C_{\mathrm{CO_2}} \quad (6)$$

$$k_{\mathrm{cm}} = k_{0\mathrm{cm},T_{\mathrm{ref}}} \exp\left[-\frac{E_{a,\mathrm{cm}}}{R}\left(\frac{1}{T}-\frac{1}{T_{\mathrm{ref}}}\right)\right] \quad (7)$$

In Eq(6), r_{cm} is the reaction rate (kmol/m^3/s), k_{cm} is the rate constant of the carbamate ion formation ((m^3/kmol)^n/s), which has the form of an Arrhenius type of equation according to Eq(7), $C_{\mathrm{NH_3}}$ and $C_{\mathrm{CO_2}}$ are the NH_3 and CO_2 concentration in the liquid phase (kmol/m^3) and n is the order of reaction with respect to NH_3.
In Eq(7), $k_{0\mathrm{cm},T_{\mathrm{ref}}}$ is the pre-exponential factor ((m^3/kmol)^n/s) and $E_{a,\mathrm{cm}}$ is the activation energy (kJ/kmol) of Reaction (5), R is the ideal gas constant (8314 Pa·m^3/kmol/K), T is the reaction temperature (K) and T_{ref} is the reference temperature (set to 298 K, the average experimental value).

3.3 Mass transfer

The CO_2 absorption rate ($N_{\mathrm{CO_2}}$, kmol/s) can be computed by means of Eq(8).

$$N_{\mathrm{CO_2}} = V a_{\mathrm{int}} K_{\mathrm{G,CO_2}} (P_{\mathrm{CO_2}} - P_{\mathrm{CO_2}}^{*}) \quad (8)$$

In Eq(8), V is the total volume of packing, a_{int} is the effective vapor-liquid interfacial area per unit of volume of packing (m^2/m^3), $K_{\mathrm{G,CO_2}}$ is the overall gas phase mass transfer coefficient for CO_2 (kmol/s/m^2/Pa), and $(P_{\mathrm{CO_2}} - P_{\mathrm{CO_2}}^{*})$ is the average driving force for mass transfer computed as the difference between the partial pressure of CO_2 in the bulk gas and the CO_2 equilibrium partial pressure of the liquid (Pa). The driving force can be computed from the experimental conditions making use of the Thomsen model.
The overall mass transfer resistance for CO_2 ($1/K_{\mathrm{G,CO_2}}$, Pa·m^2·s/mol) is the sum of the CO_2 mass transfer resistance in the gas phase and in the liquid phase, according to Eq(9).

$$\frac{1}{K_{\mathrm{G,CO_2}}} = \frac{RT}{k_{\mathrm{g,CO_2}}} + \frac{H_{\mathrm{CO_2}}}{\mathrm{E}k_{\mathrm{l,CO_2}}^{0}} \quad (9)$$

In Eq(9), $k_{\mathrm{g,CO_2}}$ and $k_{\mathrm{l,CO_2}}^{0}$ (m/s) are the CO_2 mass transfer coefficient in the gas and the liquid phase, respectively, $H_{\mathrm{CO_2}}$ is the Henry's law coefficient for CO_2 (Pa·m^3/kmol) and E is the liquid-film enhancement factor for CO_2 mass transfer due to chemical reaction. The correlations of Wang et al. (2016), obtained specifically for CO_2 capture processes with aqueous solutions as absorbents, were used to compute the vapor-liquid interfacial area and the gas-film and the liquid-film mass transfer coefficients. Transport properties for the CO_2-NH_3-H_2O system can be computed from correlations validated elsewhere (Qi et al., 2013). Consequently, $K_{\mathrm{G,CO_2}}$ and E can be computed from the experimental values of $N_{\mathrm{CO_2}}$ by means of Eq(8) and Eq(9), respectively. Considering a single irreversible reaction in the liquid phase, the enhancement factor is related to the Hatta number (Ha) and the enhancement factor assuming infinitely fast reaction (E_∞) by Eq(10), which applies for a first-order reaction as well as for a fast intermediate regime ($E > 2$ and $E_\infty > Ha/5$) (van Swaaij and Versteeg, 1992).

$$\frac{1}{(\mathrm{E}-1)^{1.35}} = \frac{1}{(\mathrm{E}_\infty-1)^{1.35}} + \left(\frac{\mathrm{Ha}}{\tanh \mathrm{Ha}} - 1\right)^{-1.35} \quad (10)$$

$$\mathrm{E}_\infty = 1 + \frac{D_{\mathrm{NH_3,L}} C_{\mathrm{NH_3,L}}}{2 D_{\mathrm{CO_2,L}} C_{\mathrm{CO_2},i}} \quad (11)$$

$$\mathrm{Ha} = \frac{\sqrt{k_{\mathrm{cm}} C_{\mathrm{NH_3,L}}^{n} D_{\mathrm{CO_2,L}}}}{k_{\mathrm{l,CO_2}}^{0}} \quad (12)$$

Under the assumptions aforementioned, Ha and E_∞ can be computed from Eq(11) and Eq(12), respectively, where $C_{\mathrm{NH_3,L}}$ and $C_{\mathrm{CO_2},i}$ are the NH_3 concentration in the bulk liquid and the CO_2 concentration at the vapor-liquid interphase (kmol/m^3), $D_{\mathrm{NH_3,L}}$ and $D_{\mathrm{CO_2,L}}$ are the diffusivities (m^2/s) in the liquid phase of NH_3 and CO_2, respectively. If the resistance for CO_2 mass transfer in the gas-film can be neglected, $C_{\mathrm{CO_2},i}$ is computed from the average CO_2 partial pressure in the bulk gas phase and $H_{\mathrm{CO_2}}$. The apparent kinetic rate constant (k_{app}, 1/s) can be computed from Eq(12) and the kinetic parameters $k_{0\mathrm{cm,T_{ref}}}$, $E_{a,cm}$ and n can be regressed making use of Eq(7) and Eq(13).

$$k_{\mathrm{app}} = k_{\mathrm{cm}} C_{\mathrm{NH_3,L}}^{n} \quad (13)$$

4. Results

In total, 82 experimental points have been obtained from the pilot plant CO_2 absorption tests simulating cement plant-like flue gas conditions, in all cases closing the component and overall mass balances within 10% of accuracy. No solids were formed in any case. Net CO_2 transfer from the gas to the liquid was obtained experimentally in all tests.

The value of the kinetic parameters of the carbamate ion formation Reaction (5) regressed in this study using the new pilot tests are shown in Table 2. Reaction (4) was neglected since its Hatta number was close to zero in all cases (the kinetic model obtained by Kucka et al. (2002) was used). Additionally, only those experimental points with a CO_2 loading in the liquid phase below 0.5 mol_{CO2}/mol_{NH3} were considered in order to assure the irreversibility of Reaction (5) (Astarita, 1967). Furthermore, the value of the apparent kinetic constant at 298 K and 5 kmol/m^3 of NH_3 in the liquid is computed with the reaction kinetics obtained in this work and, for comparison purposes, with the kinetics retrieved by Pinsent et al. (1956) (referred to as "Pinsent model"), which is the kinetic model implemented by default in Aspen Plus and broadly used in the literature for the design and optimization of CO_2 capture processes using aqueous ammonia. Apart from the higher value of the reaction rate constant obtained in this work with respect to the Pinsent model, it was found that the reaction rate order with respect to the concentration of NH_3 was between 1 and 2, instead of equals 1. This might indicate that the formation of the carbamate ion in the liquid phase at the experimental conditions tested in this work does not follow a simple two-step mechanism as proposed by the Pinsent model, but a more complex mechanism such as the termolecular or the zwitterion mechanisms (Yu el at. 2016). The discrepancies between both kinetic models may stem from the low NH_3 concentrations in the experiments used to obtain the Pinsent model, below 0.19 mol/L in all cases.

On the other hand, CO_2 capture efficiencies as high as 65% and a minimum NH_3 concentration in the outlet gas stream of 10,000 ppm_v were achieved at NH_3 concentrations in the liquid of 10 mol_{NH3}/mol_{water} with a 3 m high packing, while decreasing the NH_3 concentration in the liquid down to 4 mol_{NH3}/mol_{water} allowed to limit the NH_3 concentration in the outlet gas to 2,000 ppm_v achieving CO_2 capture efficiencies up to 30%. Experimentally, it has been observed that higher $C_{\mathrm{NH_3}}$ and lower $l_{\mathrm{CO_2}}$ lead to a desirable increase of the CO_2 capture efficiency, as shown in Figure 4, but increases the NH_3 slip. Consequently, the optimization of the operating conditions of the industrial CO_2 absorber will require the consideration of these opposing effects. In addition, the CO_2 absorption rate increased with a higher CO_2 partial pressure in the inlet flue gas. In general, the model obtained in this study is able to reproduce the CO_2 capture efficiency (ψ_{CO_2}) obtained experimentally, as shown in Figure 4.

Table 2: Kinetic parameters of the carbamate ion reaction

Model	n $[-]$	$E_{\mathrm{a,cm}}$ [kJ/kmol]	$k_{\mathrm{cm}}(T = T_{\mathrm{ref}} = 298\ \mathrm{K})$ $[(\mathrm{m^3/kmol})^n \cdot \mathrm{s^{-1}}]$	$k_{\mathrm{app}}(T = T_{\mathrm{ref}} = 298\ \mathrm{K}; C_{\mathrm{NH_3}} = 5\ \mathrm{kmol/m^3})$ $[\mathrm{s^{-1}}]$
This work	1.32	30,100	162	1,356
Pinsent	1	48,500	431	2,155

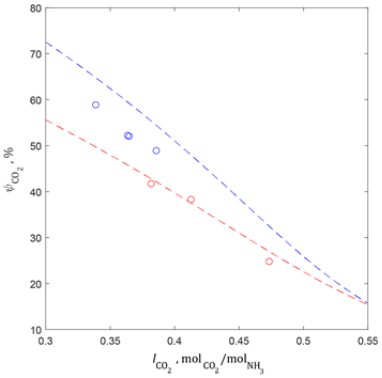

Figure 4: Effect of the NH_3 concentration and CO_2 loading of the liquid on the CO_2 capture efficiency for some representative experiments of Campaign 2. Points are experimental results while the lines account for the prediction of the model developed in this work. Experimental conditions: $T_L = 18\,°C$, $L^{in}/G^{in} = 8.6\,kg/kg$, $v_{s,G} = 1\,m/s$, $p^{in}_{CO_2,G} = 20\,kPa$, (red) $C_{NH_3} = 6\,mol_{NH_3}/kg_{water}$, (blue) $C_{NH_3} = 10\,mol_{NH_3}/kg_{water}$.

5. Conclusions

The rate-based model developed in this work can be used with engineering purposes for the design and optimization of the CO_2 capture process with aqueous ammonia applied to cement plants. Since the model is able to reproduce the experimental evidence regarding solid formation, the design and optimization of the CO_2 capture process can be constrained to those operating conditions that avoid the formation of solids and, therefore, the clogging of the packing.

Acknowledgments

This project has received funding from the European Union's Horizon 2020 research and innovation programme under grant agreement No 641185. This work was supported by the Swiss State Secretariat for Education, Research and Innovation (SERI) under contract number 15.0160. The results in this publication reflect only the authors' view. The European Commission is not responsible for any use that may be made of the contents.

References

Astarita G. Mass Transfer with Chemical Reaction, Elsevier, Amsterdam, 1967.

Baburao B., Kniesburger P., Lombardo G., 2015, Chilled Ammonia Process Operation and Results from Pilot Plant at Technology Centre Mongstad. Presentation at TCCS-8, Trondheim, Norway.

Darde V., van Well W.J.M., Stenby E.H., Thomsen K., 2010, Modeling of carbon dioxide absorption by aqueous ammonia solutions using the Extended UNIQUAC model, Industrial & Engineering Chemistry Research, 49, 12663-12674.

Jänecke E., 1929, Über das System H2O, CO2 und NH3,. Zeitschrift für Elektrochemie, 35, 716-728.

Kucka L., Kenig E.Y., Górak A., 2002, Kinetics of the Gas-Liquid Reaction between Carbon Dioxide and Hydroxide Ions. Industrial & Engineering Chemistry Research, 41, 5952-5957.

Pérez-Calvo J.-F., Sutter D., Gazzani M., Mazzotti M., 2017, Application of a Chilled Ammonia-based Process for CO2 Capture to Cement Plants, Energy Procedia, 114, 6197-6205.

Pinsent B.R.W., Pearson L., Roughton F.J.W., 1956, The kinetics of combination of carbon dioxide with ammonia. Transactions of the Faraday Society, 52, 1594-1598.

Qi G., Wang S., Yu H., Wardhaugh L., Feron P., Chen C., 2013, Development of a rate-based model for CO2 absorption using aqueous NH3 in a packed column. International Journal of Greenhouse Gas Control, 17, 450-461.

Que H., Chen C.-C., 2011, Thermodynamic Modeling of the NH3-CO2-H2O System with Electrolyte NRTL Model, Industrial & Engineering Chemistry Research, 50, 11406-11421

Sutter D., Gazzani M., Mazzotti M., 2015, Formation of solids in ammonia-based CO2 capture processes – Identification of criticalities through thermodynamic analysis of the CO2-NH3-H2O system, Chemical Engineering Science, 133, 170-180.

van Swaaij W.P.M., Versteeg G.F., 1992, Mass Transfer Accompanied With Complex Reversible Chemical Reactions In Gas-Liquid Systems: An Overview, Chemical Engineering Science, 47, 3181-3195

Wang C., Song D., Seibert F.A., Rochelle G.T., 2016, Dimensionless Models for Predicting the Effective Area, Liquid-Film, and Gas-Film Mass-Transfer Coefficients of Packing, Industrial & Engineering Chemistry Research, 55, 5373-5384.

Yu H., Morgan S., Allport A., Cottrell A., Do T., McGregor J., Wardhaugh L., Feron P., 2011, Results from trialling aqueous NH3 based post-combustion capture in a pilot plant at Munmorah power station: Absorption. Chemical Engineering Research and Design, 89, 1204-1215.

Yu H., Tan Z., Thé J., Feng X., Croiset E., Anderson W.A., 2016, Kinetics of the Absorption of Carbon Dioxide into Aqueous Ammonia Solutions. AIChE Journal, 62, 3673-3684.